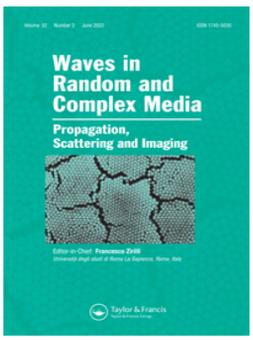

Taylor & Francis
Taylor & Francis Group

Waves in Random and Complex Media

ISSN: (Print) (Online) Journal homepage: https://www.tandfonline.com/loi/twrm20

Unsteady magnetohydrodynamic nanofluid flow over a permeable exponentially surface manifested with non-uniform heat source/sink effects

G. Vinod Kumar, Khalil Ur Rehman, R.V.M.S.S.K. Kumar & Wasfi Shatanawi

To cite this article: G. Vinod Kumar, Khalil Ur Rehman, R.V.M.S.S.K. Kumar & Wasfi Shatanawi (2022): Unsteady magnetohydrodynamic nanofluid flow over a permeable exponentially surface manifested with non-uniform heat source/sink effects, Waves in Random and Complex Media, DOI: 10.1080/17455030.2022.2072531

To link to this article: https://doi.org/10.1080/17455030.2022.2072531

Published online: 17 May 2022.

WAVES IN RANDOM AND COMPLEX MEDIA
https://doi.org/10.1080/17455030.2022.2072531

Taylor & Francis
Taylor & Francis Group

Unsteady magnetohydrodynamic nanofluid flow over a permeable exponentially surface manifested with non-uniform heat source/sink effects

G. Vinod Kumar[a], Khalil Ur Rehman[b,c], R.V.M.S.S.K. Kumar[d] and Wasfi Shatanawi[b,e]

[a]Department of Mathematics, CSSR & SRRM Degree and PG College, Kamalapuram, India; [b]Department of Mathematics and Sciences, College of Humanities and Sciences, Prince Sultan University, Riyadh, Saudi Arabia; [c]Department of Mathematics, Air University, Islamabad, Pakistan; [d]Department of Mathematics, Government Polytechnic College, Ananthapur, India; [e]Department of Mathematics, Faculty of Science, The Hashemite University, Zarqa, Jordan

ABSTRACT

Current research inspects the influences of two-dimensional unsteady nanofluid flow over a permeable exponential stretching sheet with the impact of magnetic field parameter, thermal radiation together with a non-uniform heat source or sink. The dimensional equations namely Partial differential equations (PDE's) are transformed into dimensionless form as ordinary differential equations (ODE's) by using the suitable transformations. The reframed ODE's are solved numerically through the computer-based tool MATLAB with the bvp4c package. The derived results of velocity, temperature and species distributions are depicted graphically. Also, the numerical results of skin friction coefficients, heat transfer rate and mass transfer rate in terms of Nusselt number and Sherwood number are deployed via tables. The comparison of the present work with published work shows complete agreement for skin friction factor and Nusselt number. In absolute sense skin friction enhances as magnetic field parameter enhances. The Brownian motion and thermophoresis parameters play an essential role towards thermophysical flow field of nanofluids. Further, we noticed that both Brownian motion parameter and thermophoresis parameter cause an enhancement in the fluid temperature. Furthermore, the unsteady parameter causes increase in wall friction and heat transfer rate. However, the opposite trend is observed for the heat source/sink parameters.

ARTICLE HISTORY
Received 4 October 2021
Accepted 26 April 2022

KEYWORDS
Nanofluid; thermal radiation; exponential stretching sheet; heat source or sink

Nomenclature

(u, v)	Velocity components in (x, y)directions
B_0	Magnetic field strength
T	Dimensional temperature
C	Dimensional concentration
C_p	Heat capacity at constant pressure

CONTACT Khalil Ur Rehman khalil.rehman@mail.au.edu.pk

υ	Kinematic viscosity
ρ	Fluid density
R	Radiation parameter
A	Unsteady parameter
S	Suction/Injection parameter
τ	Ratio of specific heats
D_B	Coefficient of Brownian motion
D_T	Coefficient of Thermophoresis diffusion
κ	Thermal conductivity
Pr	Prandtl number
M	Magnetic field parameter
Nb	Brownian motion parameter
Nt	Thermophoresis parameter
L	Characteristic length
A^*, B^*	Heat sink or source parameters
Cf	Skin friction coefficient
Nu_x	Rate of local heat transfer coefficient
Sh_x	Rate of local mass transfer coefficient
Sc	Schmidt number
q_w	Heat flux
q_m	Mass flux
Re_x	Local Reynolds number

Greek Symbols

η	Similarity variable
σ	Electrical conductivity
α_T	Thermal diffusivity
θ	Dimensionless temperature
ϕ	Dimensionless concentration
τ_w	Shear stress
μ	Dynamic viscosity

Subscripts

∞	Ambient condition
w	Condition on the sheet or wall

Superscript

$'$	Differentiation w.r.t η
$*$	Dimensional properties

1. Introduction

The boundary layer flow of a viscous fluid with heat transfer along the flat surface was being used at the industrial works like hot rolling, extrusion of metal, frequent elaboration of plastic films and the wires drawing. Many researchers spent their work investigating a flow field. Sakiadis [1] was a pioneer in investing the boundary layer flow along the stretched surface, attaining the fixed velocity with improving the boundary layer equations for axisymmetric flows in 2D. Erickson et al. [2] prolonged the Sakiadis concept [1], implementing the forces injection and suction upon a stretched surface stirring with stable velocity also examined the impact on the fluid flow and heat transfer. Plenty of physical conditions related to movable stretching sheet attaining the fixed velocity under various thermal conditions have been examined by Carragher and Crane [3], Grubka and Bobba [4], Magyari and Keller [5] and Mabood et al. [6] discussed the hydromagnetic flow over an exponentially stretching sheet with radiation. The hydromagnetic boundary layer flow over an exponentially stretching sheet with heat transfer embedded in a stratified medium was analyzed by Mukhopadhyay [7]. Also, the researchers Hayat et al. [8] investigated the unsteady boundary layer flow over an exponentially stretching sheet with slip conditions and in the presence of the magnetic field. They found that the slip parameters reduce the boundary layer thickness. The researchers [9–13] have reported a few useful recent investigations over an exponentially stretching sheet.

Conventional heat transfer fluids like molten salts, oil, water, gases, etc., have inherently poor thermal conductivity compared to solids. So, these possess limited heat transfer capability, which is inadequate to handle modern cooling systems. With this intention, Choi [14] gained the interest to propose an innovative idea of transforming convectional heat transfer fluids to sophisticated heat transfer fluids and named them nanofluids, which are prepared by pouring the nanoparticles into conventional fluids having a diameter of less than 100 nm. The nanofluids have high cooling capabilities and show an abnormal high thermal conductivity compared to natural convectional heat fluids. These are extensively used in automotive engines, cooling chips, preventing clogging problems in micro-channels, and helpful in drug delivery, and the pharmaceutical industry makes giant leaps and bounds. Later, Buongiorno [15] and Tiwary and Das [16] developed two nanofluid models, namely homogeneous and non-homogeneous. Buongiorno [15], in his model, has proposed that seven mechanisms affect the nanofluid flow, of which only Brownian diffusion and thermophoresis are predominant mechanisms. Due to its numerous applications, the following researchers studied nanofluid flows. The 2D boundary layer flow of a nanofluid over an exponentially stretching sheet with suction/injection is analyzed by Nadeem and Lee [17]. The effect of Brownian motion and thermophoresis on boundary layer flow over an exponentially stretching sheet with convective boundary condition is discussed by Mustafa et al. [18]. Nadeem et al. [19] considered the three-dimensional water-based nanofluid flow over an exponentially stretching sheet. They found that the temperature exponent parameter reduces the heat transfer rate. They found that the convection parameters improve the nanofluid temperature and heat transfer rate. Bhattacharyya and Layek [20] analyzed the flow of magnetohydrodynamic nanofluid along the permeable exponentially stretching sheet. Anwar et al. [21] discussed the stagnation point flow of a nanofluid past an exponentially stretching sheet with the influence of a magnetic field and thermal radiation. Loganathan and Vimala [22] studied the hydromagnetic boundary layer flow of a nanofluid

theoretically through the exponentially stretching sheet with the radiation effect. In this study, they used four types of nanoparticles with the base fluid water. They found that TIO_2 nanofluid has better enhancement on heat transfer compared to *Cu*, *Ag* and *S* water-based nanofluids. The magnetohydrodynamic flow of a water-based nanofluid over a permeable exponentially stretching sheet with convective type boundary conditions was discussed by Hayat et al. [23]. They concluded that the convection parameter improves the heat transfer rate. Mohamed et al. [24] discussed the hydromagnetic radiative nanofluid flow over an exponentially stretched sheet in a medium that consists of porous with the effects like suction or injection.

The examination of the temperature field as customized either by generation or the absorption of heat in the moving fluids is predominant in the aspects of several physical problems, such as chemical reaction processes or in the problems associated with dissociating fluids. The volumetric rate of heat generation is treated as a constant or function of space variables, whilst few other studies also directly considered frictional heating and the expansion effect. Foraboschi and Federicol [25] assumed volumetric rate of heat generation of the type $Q = Q_o(T - T_0)$ when $T \geq T_0$ and $Q = 0$ when $T < T_0$. Very recently, the authors Shahzad et al. [26] studied the flow analysis of a Jeffery nanofluid over a stretchable surface with the influence of a magnetic field and viscous dissipation. The authors concluded that graphene-EG nanofluid temperature is higher than the conventional fluid temperature. Later, the investigators Shamshuddin and Mohamed [27] examined the heat transfer phenomena of a magnetized nanofluid flow over a spinning disc in the presence of variable viscosity and variable thermal conductivity. In this investigation, the authors considered the water-based nanofluid containing ferromagnetic particles. Amine et al. [28] examined the behavior of a triangular cavity occupied with the water – based Ag/MgO hybrid nanofluid in the presence of a magnetic field and quarter circular porous medium. The numerical and analytical investigation of a mixed convection Falkner-Skan flow of a nanofluid over a vertical plate was studied by Boumaiza et al. [29]. Waqas et al. [30] examined the gyrotactic motile microorganisms' effects of a Jeffery nanofluid over a stretching sheet influenced by a magnetic dipole with ferromagnetic particles. They found that the Ferro-liquid, the buoyancy ratio, and retardation parameters are causes to retard the fluid velocity.

The present adopted one-phase nanofluid model particularly reveals that the type of application affects the behavior of nanofluids in such a way as now the structure of the energy equation alters in the context of this adopted methodology.

As per the authors' knowledge, no effort has been found to study the nanofluid flow along a permeable exponentially stretching sheet with the effects like non-uniform heat source or sink and the impact of radiation. The thermophoresis and Brownian motion effects are considered. The ordinary differential equations are solved numerically. The impact of involved parameters on flow field is examined and offered by using tables and graphs.

2. Mathematical formulation

We consider an incompressible two-dimensional unsteady nanofluid flow through an exponentially permeable stretching sheet in the existence of thermal radiation, magnetic field,

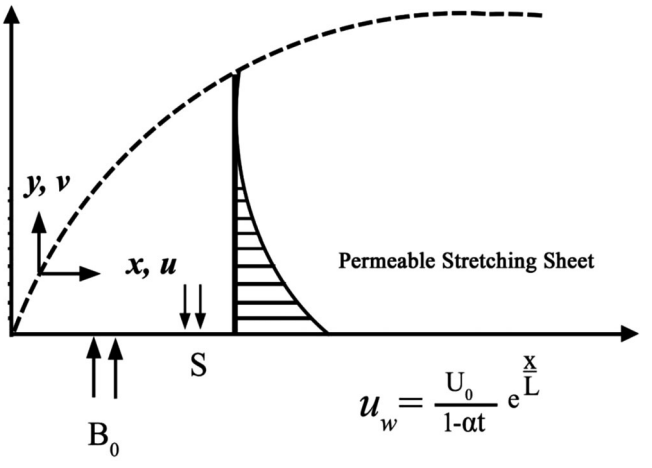

Figure 1. Physical representation and co-ordinate system.

also non-uniform heat source/sink effects. The flow is caused via an exponentially stretching sheet, see Figure 1. The flow of fluid is limited to $y > 0$.

- It is taken that the sheet is exponentially stretched and have velocities $u_w(x,t) = \frac{U_0}{1-\alpha_1 t} e^{\frac{x}{L}}$ and $v_w(x,t) = \frac{V_0}{1-\alpha_1 t} e^{\frac{x}{2L}}$ [31]. Here $U_0 > 0$, is the shrinking constant and $U_0 < 0$ is the stretching constant, $V_0 < 0$ for mass suction and $V_0 > 0$ corresponds to mass injection.
- A variable Magnetic field $B(x,t) = \frac{B_0}{\sqrt{1-\alpha_1 t}} e^{\frac{x}{2L}}$ [31] is applied normal to flow direction.
- The unsteady flow starts at $t = 0$.
- The suction is applied normal to the sheet.
- In addition to this, the effects of thermal radiation and non-uniform heat source/sink are taken into account.
- The non-homogeneous nanofluid model namely Buongiorno model has been considered to study the mutual impacts of Nt and Nb.

Under the aforesaid assumptions the time-dependent governing boundary layer approximations are

$$\frac{\partial u}{\partial x} + \frac{\partial v}{\partial y} = 0, \tag{1}$$

$$\frac{\partial u}{\partial t} + u\frac{\partial u}{\partial x} + v\frac{\partial v}{\partial y} = \upsilon\frac{\partial^2 u}{\partial y^2} - \frac{\sigma {B_0}^2}{\rho}u, \tag{2}$$

$$\frac{\partial T}{\partial t} + u\frac{\partial T}{\partial x} + v\frac{\partial T}{\partial y} = \alpha_T\frac{\partial^2 T}{\partial y^2} + \tau\left\{D_B\frac{\partial C}{\partial y}\frac{\partial T}{\partial y} + \frac{D_T}{T_\infty}\left(\frac{\partial T}{\partial y}\right)^2\right\} - \frac{1}{\rho C_P}\frac{\partial q_r}{\partial y} + \frac{q'''}{\rho C_P}, \tag{3}$$

$$\frac{\partial C}{\partial t} + u\frac{\partial C}{\partial x} + v\frac{\partial C}{\partial y} = D_B\frac{\partial^2 C}{\partial y^2} + \frac{D_T}{T_\infty}\frac{\partial^2 T}{\partial y^2}. \tag{4}$$

The appropriate boundary conditions are

$$\begin{aligned} &u = u_w(x,t),\ v = v_w(x,t),\ T = T_w(x,t),\ C = C_w(x,t) \quad \text{at } y = 0,\\ &u \to 0,\ T \to T_\infty,\ C \to C_\infty \qquad\qquad\qquad\qquad \text{as } y \to \infty. \end{aligned} \tag{5}$$

The non-uniform heat source/sink is modeled as [32]

$$q''' = \frac{\kappa u_w}{x\upsilon}[A^*(T_w - T_\infty)\mathrm{f}' + B^*(T - T_\infty)], \tag{6}$$

and,

$$T_w = T_\infty + T_0\left(\frac{e^{\frac{x}{2L}}}{1-\alpha_1 t}\right) \text{and } C_w = C_\infty + C_0\left(\frac{e^{\frac{x}{2L}}}{1-\alpha_1 t}\right) \tag{7}$$

The following are the similarity variables

$$\begin{aligned} u &= \frac{U_0}{1-\alpha_1 t}e^{\frac{x}{L}}\mathrm{f}',\ \ v = -\left(\sqrt{\frac{U_0\upsilon}{2L(1-\alpha_1 t)}}e^{\frac{x}{2L}}\right)(\mathrm{f} + \eta\mathrm{f}'),\\ \theta &= \frac{T - T_\infty}{T_w - T_\infty},\ \ \phi = \frac{C - C_\infty}{C_w - C_\infty},\ \ \eta = y\sqrt{\frac{U_0}{2\,\upsilon L\,(1-\alpha_1 t)}}\,e^{\frac{x}{2L}}. \end{aligned} \tag{8}$$

Use of Equation (8) into Equations (2)–(5) brings

$$\mathrm{f}''' - \mathrm{M}\mathrm{f}' - 2\mathrm{A}\mathrm{f}' - \mathrm{A}\eta\mathrm{f}'' - 2\mathrm{f}'^2 + \mathrm{f}\mathrm{f}'' = 0 \tag{9}$$

$$\left(1 + \frac{4\mathrm{R}}{3}\right)\theta'' + \mathrm{Pr}(\mathrm{Nb}\theta'\phi' + \mathrm{Nt}\theta'^2 - 2\mathrm{A}\theta - \mathrm{A}\eta\theta' + \mathrm{f}'\theta - \mathrm{f}\theta') + 2(\mathrm{A}^*\mathrm{f}' + \mathrm{B}^*\theta) = 0 \tag{10}$$

$$\phi'' + \frac{\mathrm{Nt}}{\mathrm{Nb}}\theta'' - Sc\,(2\mathrm{A}\phi + \mathrm{A}\eta\,\phi' + \mathrm{f}'\phi - \mathrm{f}\phi') = 0 \tag{11}$$

The corresponding boundary conditions are

$$\begin{aligned} &\mathrm{f}'(\eta) = 1,\ \mathrm{f}(\eta) = \mathrm{S},\ \ \theta(\eta) = 1,\ \ \phi(\eta) = 1, \quad \text{at } \eta = 0\\ &\mathrm{f}'(\eta) = 0,\ \ \theta(\eta) = 0,\ \ \phi(\eta) = 0, \qquad\qquad \text{as } \eta \to \infty \end{aligned} \tag{12}$$

The flow parameters in the Equations (9)–(11) are defined as follows

$$\begin{aligned} &\mathrm{M} = \frac{\sigma {B_0}^2}{\rho U_0},\ \ \mathrm{Pr} = \frac{\upsilon}{\alpha_T},\ \ \mathrm{A} = \frac{\alpha_1 L\, e^{\frac{-x}{L}}}{U_0},\ \ Sc = \frac{\upsilon}{D_B},\ \ \mathrm{R} = \frac{4\sigma^* T_\infty^3}{\kappa k^*}\\ &\mathrm{Nb} = \tau\frac{D_B(C_w - C_\infty)}{\upsilon},\ \ \mathrm{Nt} = \tau\frac{D_T(T_w - T_\infty)}{\upsilon T_\infty},\ \ \mathrm{S} = V_0\sqrt{\frac{2L\upsilon}{U_0(1-\alpha_1 t)}} \end{aligned} \tag{13}$$

The important physical parameters at the surface are the coefficient of skin-friction, the Nusselt number and the local Sherwood number are mathematically expressed as

$$Cf = \frac{2\tau_w}{\rho u_w^2},\ Nu_x = \frac{xq_w}{\kappa(T_w - T_\infty)} \text{ and } Sh_x = \frac{xq_m}{D_B(C_w - C_\infty)} \tag{14}$$

where τ_w is the shear stress, q_w and q_m are the wall heat flux and mass flux respectively, and are defined as

$$\tau_w = \mu\left(\frac{\partial u}{\partial y}\right)_{y=0}, q_w = -\kappa\left(\frac{\partial T}{\partial y}\right)_{y=0} \text{ and } q_m = -D_B\left(\frac{\partial C}{\partial y}\right)_{y=0} \tag{15}$$

Substituting Equations (7) and (15) in Equation (14), we have

$$\left(\frac{Re_x}{2}\right)^{\frac{1}{2}} Cf = \mathrm{f}''(0),\ \left(\frac{Re_x}{2}\right)^{\frac{-1}{2}} Nu_x = -\frac{x}{L}\left(1 + \frac{4\mathrm{R}}{3}\right)\theta'(0), \text{ and } \left(\frac{Re_x}{2}\right)^{\frac{-1}{2}} Sh_x = -\frac{x}{L}\phi'(0). \tag{16}$$

where Re_x, is the local Reynolds number.

3. Method of solution

The differential Equations (9)–(11) and related boundary conditions (12) cannot be solved analytically, so they are solved numerically using the MATLAB tool with the default bvp4c package. In general, the MATLAB software accompanied the built-in shooting technique. Meanwhile, the choice of mesh scaling and error mechanism is equipped by the residual of continuous solution. The approval was fixed up to 10^{-7}. In this problem, the conclusion is guaranteed ($\eta_\infty = 5$) that all the numerical solution accurately approaches to the asymptotic values. The flow chart for adopted methodology is shown in Figure 2. One can access the adopted methodology detail in Refs. [33,34] and some other schemes to narrate the fluid flow narrating differential equations in Refs. [37–45].

4. Result and discussions

The impact of various flow quantities is analyzed and discussed through Figures 3–15. Also, the friction factor coefficient at the wall and the rates of heat and mass transfer coefficients are presented in Table 3. For the correctness of the method, the results are verified with existing results and are to be found very good with Magyari and Keller [5], Mabood et al. [6], Ishak [12], Jat and Chand [13], El-Aziz [35] and Mukhopadhyay [36] (see Table 1 and Table 2). Throughout the calculations the default parameters are taken as $\mathrm{M} = 2,\ \mathrm{A} = \mathrm{A}^* = \mathrm{B}^* = \mathrm{Nb} = 0.2, \mathrm{Nt} = 0.3,\ Sc = 0.3, \mathrm{Pr} = 0.71,\ \mathrm{S} = 0.6, \mathrm{R} = 0.5$ and $\eta = 5$.

Table 1. Comparison of $-\mathrm{f}''(0)$ against various values of M.

	M			
	0	0.5	1.0	2.0
Jat and Chand [13]	−1.2903770	−1.4695040	−1.6303845	−1.9128497
Present results	−1.290377	−1.469504	−1.630384	−1.912850

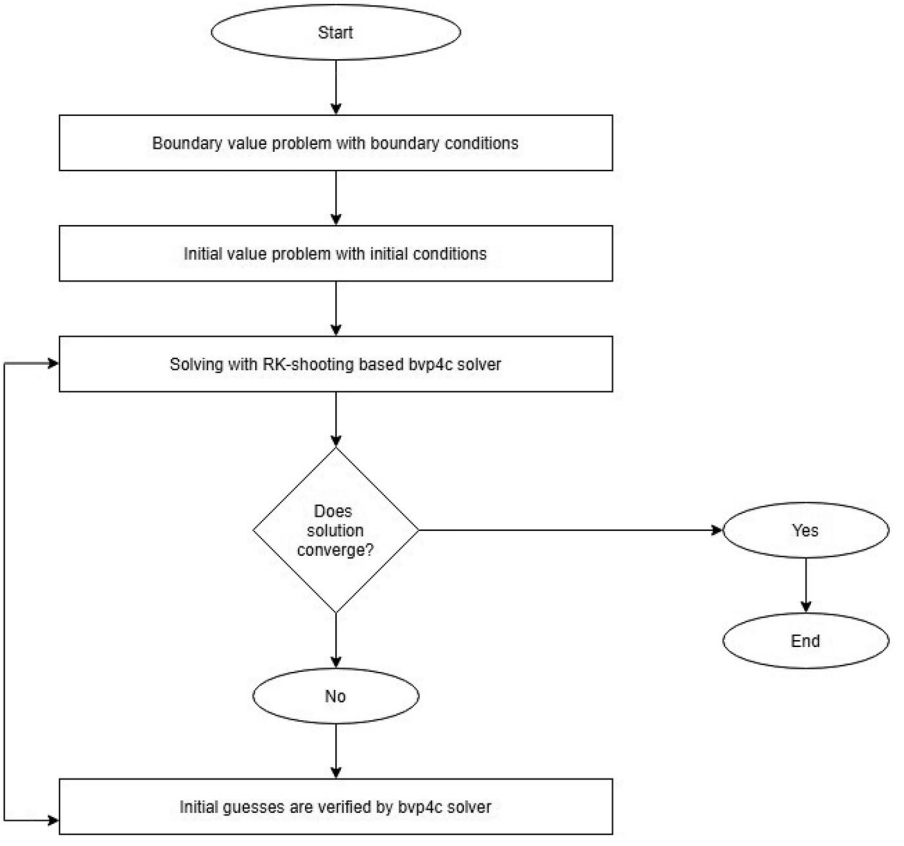

Figure 2. Flow chart describing the MATLAB simulation process.

Table 2. Comparison of heat transfer coefficient $-\theta'(0)$ for various values of M, Pr, R with $A = \eta = R = Nb = Nt = A^* = B^* = Sc = S = 0$.

R	M	Pr	Magyari and Keller [5]	Mabood et al. [6]	Ishak [12]	El-Aziz [35]	Mukhopadhyay [36]	Present Results
0	0	1	0.9548	0.95478	0.9548	0.9548	0.9547	0.954853
–	–	2	–	1.47151	1.4715	–	1.4714	1.471445
–	–	3	1.8691	1.86909	1.8691	1.8691	1.8691	1.869062
–	–	5	2.5001	2.50012	2.5001	2.5001	2.5001	2.500121
–	–	10	3.6604	3.66039	3.6604	3.6604	3.6603	3.660344
1	0	1	–	0.53121	0.5312	–	0.5312	0.531425
0	1	1	–	0.86113	0.8611	–	0.8610	0.861126
0.5	0	2	–	1.07352	–	1.0735	1.0734	1.073524
		3	–	1.38075	–	1.3807	1.3807	1.380710
1	0	3	–	1.12142	–	1.1214	1.1213	1.121403
1	1	1	–	0.4505	0.4505	–	0.4505	0.451164

The effect of the magnetic field parameter on the velocity and temperature distributions is depicted in Figure 3 and Figure 4. From Figure 3, it is seen that when we increase magnetic field parameter M = 1,2,3 and 4, the velocity of fluid decreases. This impact is due to activation of Lorentz force. Higher values of magnetic field parameter enhance the Lorentz force and as a result fluid particles faced resistance, which leads to decline values

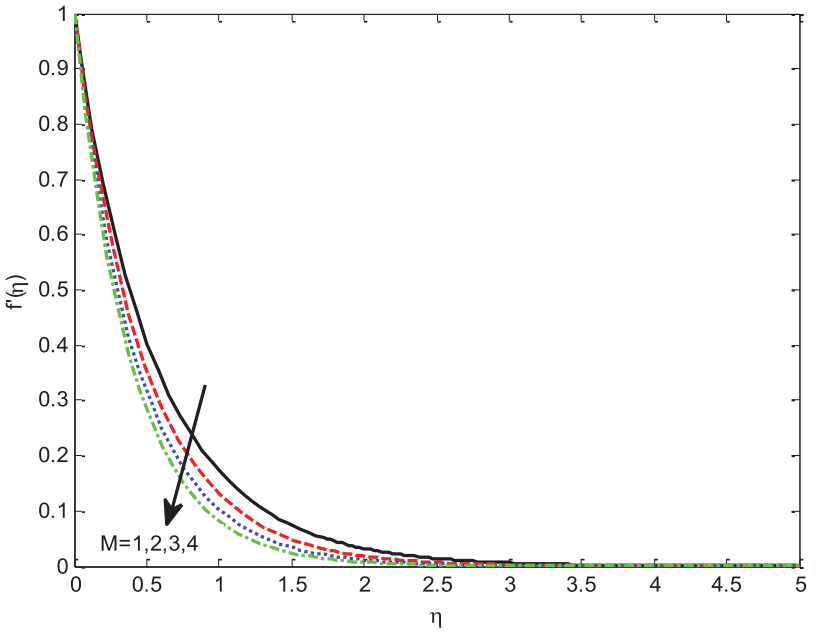

Figure 3. Effect of M on $f'(\eta)$.

of velocity. But the opposite trend is perceived in the temperature field when we increase magnetic field parameter M $= 1,2,3$ and 4. Resistance offered to fluid particles generate heat energy as result, the temperature of fluid increases. Figures 5–7 display the variations in velocity, temperature and concentration distribution of a fluid towards unsteady parameter. These figures emphasize that all the distributions are diminished with the imposition of an unsteady parameter A $= 1,2,3$ and 4. This is because the velocity along the sheet reduces with the rise in the value of A and also, less heat is transferred from the fluid to the sheet, so that the temperature decreases as well the similar result has been detected for fluid concentration also. The impact of heat generation parameter on fluid temperature is examined and offered by way of Figure 8. We observed that when we increase the heat generation parameter $A^* = 0.1, 0.2, 0.3$ and 0.4, the temperature of fluid increases.

This is because higher values of heat generation parameter produce heat energy and as a result temperature increases. It is apparent from Figure 9 that the fluid velocity is suppressed with escalating values of a suction parameter. Physically, the suction parameter is a mediator that causes resistance to the fluid flow to decrease the fluid velocity. Also, fluid temperature decreases with increasing values of S, which is explored in Figure 10. The impact of Brownian motion parameter (Nb) on fluid temperature and concentration is presented in Figure 11 and Figure 12, and noticed that escalating the values of Nb inflates the fluid temperature. Since the role of Brownian motion is dominant in enhancing the thermal conductivity of nanofluids, more heat transfer occurs and makes the temperature of fluid increase. Also, an increase in Nb the unsystematic motion and collision of the minute particles of the fluid enhances and then declines the nanoparticle concentration. Figure 13 and Figure 14 elucidated the influence of the thermophoresis parameter (Nt) on temperature and nanoparticle concentration. It is clear that both the temperature and concentration of

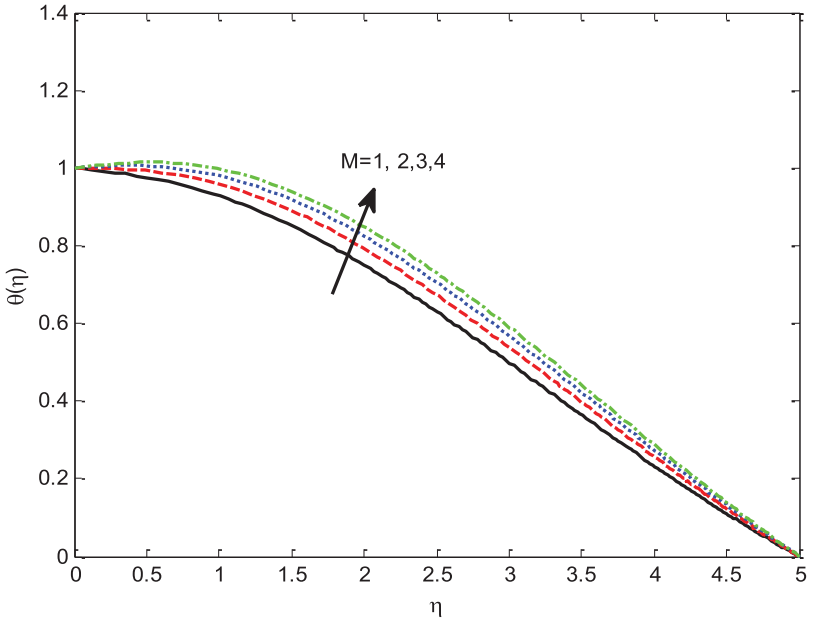

Figure 4. Effect of M on $\theta(\eta)$.

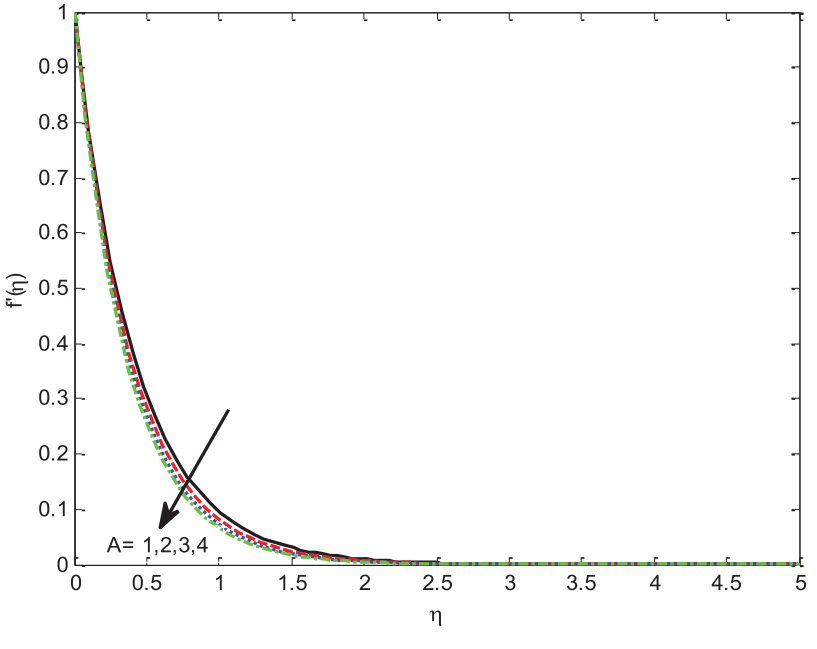

Figure 5. Effect of A on $f'(\eta)$.

fluid increase with an increase in Nt. Physically, thermophoresis is a mechanism of pulling small particles away from hot to cold surfaces. As a result, it intensifies the fluid temperature. For larger value of Nt coincides with the stronger thermophoretic diffusion that blows the

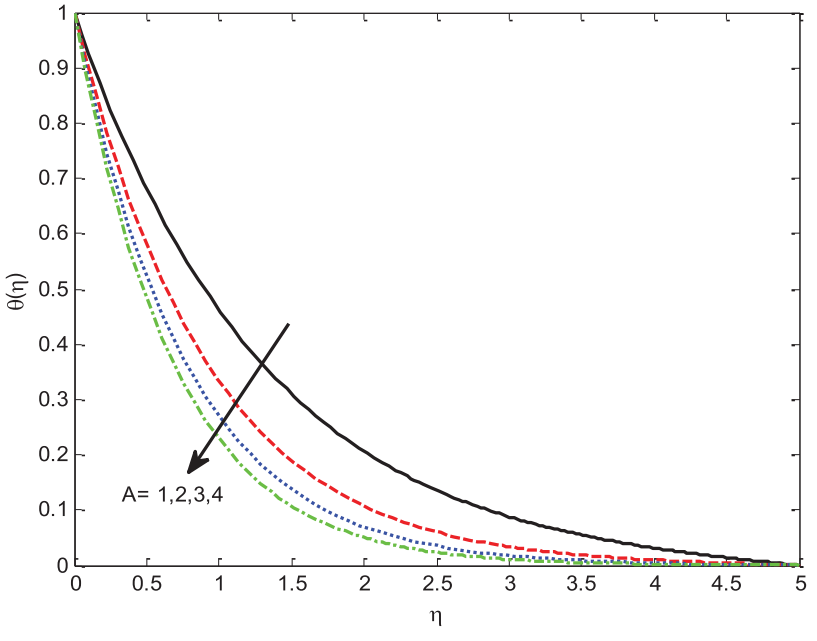

Figure 6. Effect of A on $\theta(\eta)$.

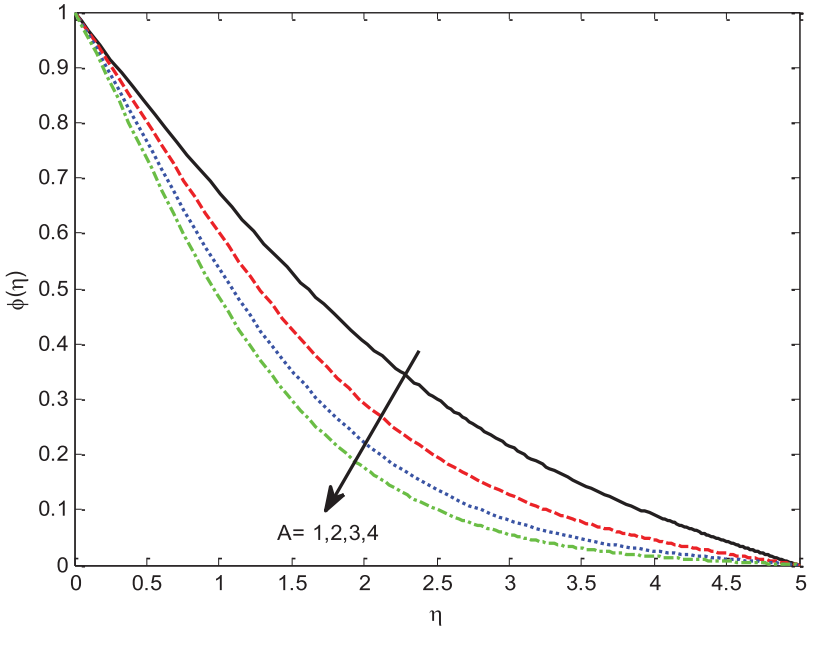

Figure 7. Effect of A on $\phi(\eta)$.

nanoparticles out from the surface of hot to cold ambient fluid. So, the nanoparticle concentration is increased. The impact of radiation parameter (R) on temperature is offered in Figure 15. Increasing the values of R release more heat energy into the flow and dominant

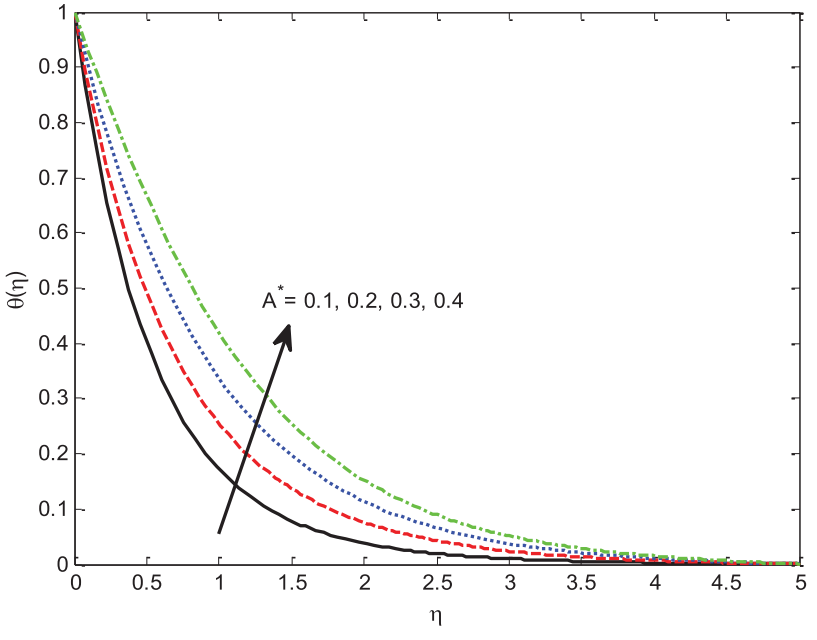

Figure 8. Effect of A* on $\theta(\eta)$.

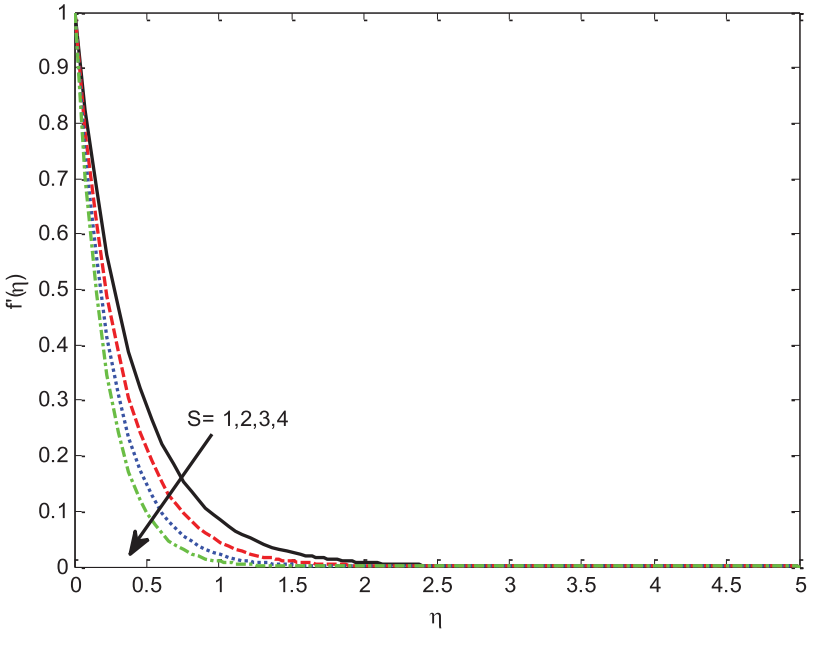

Figure 9. Effect of S on $f'(\eta)$.

effects over conduction, so that the temperature of fluid escalates with improving values of R.

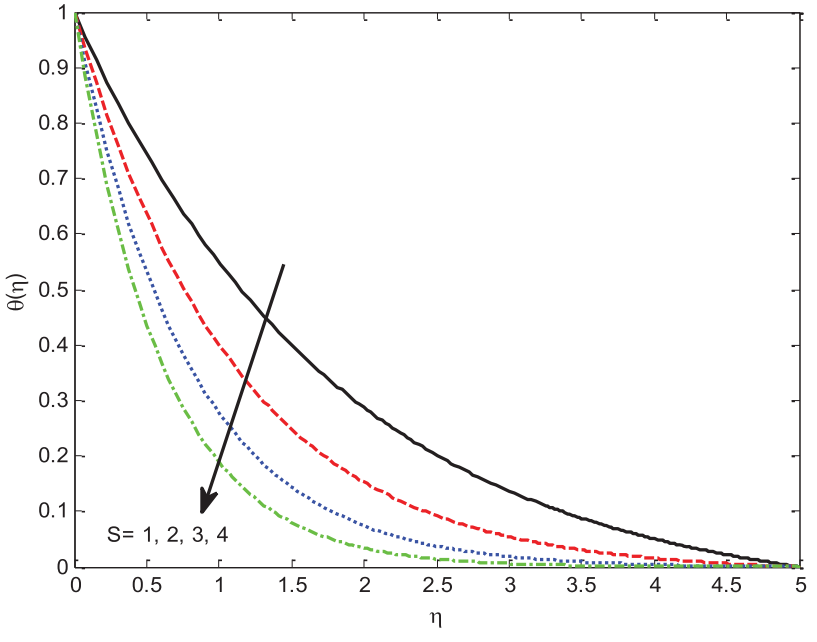

Figure 10. Effect of S on $\theta(\eta)$.

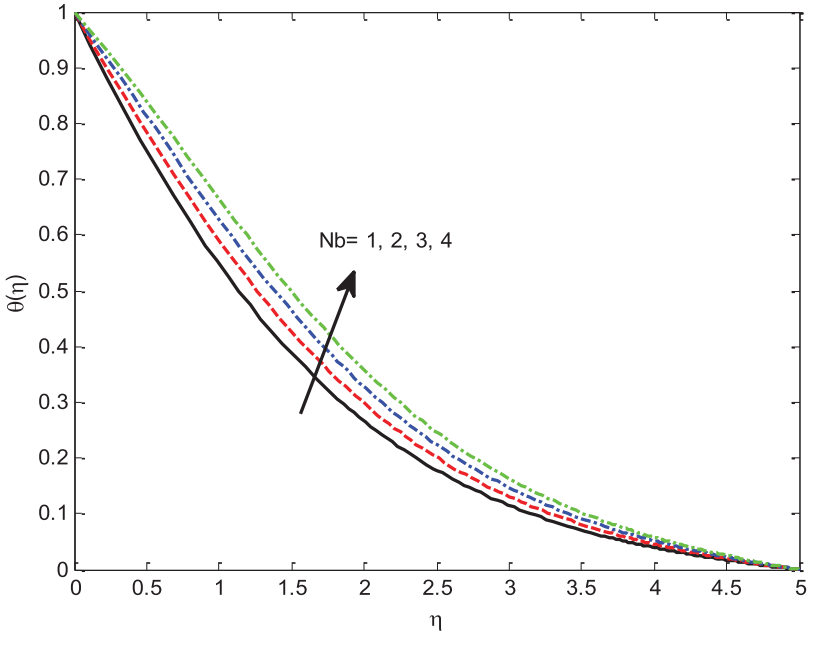

Figure 11. Effect of Nb on $\theta(\eta)$.

Table 1 and Table 2 present the comparison values of the friction factor coefficient and heat transfer coefficient at the wall with the existing results of Magyari and Keller [5], Mabood et al. [6], Ishak [12], Jat and Chand [13], El-Aziz [35] and Mukhopadhyay [36] and in

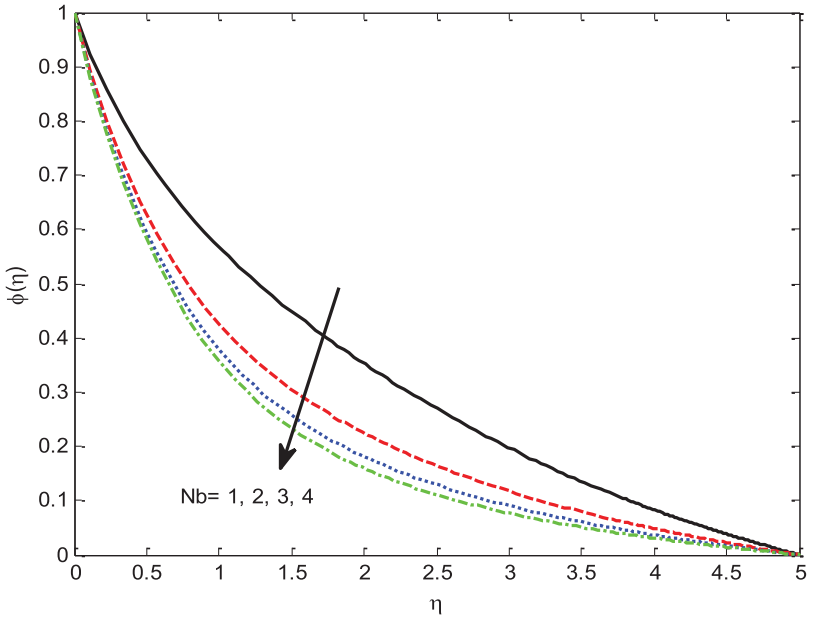

Figure 12. Effect of Nb on $\phi(\eta)$.

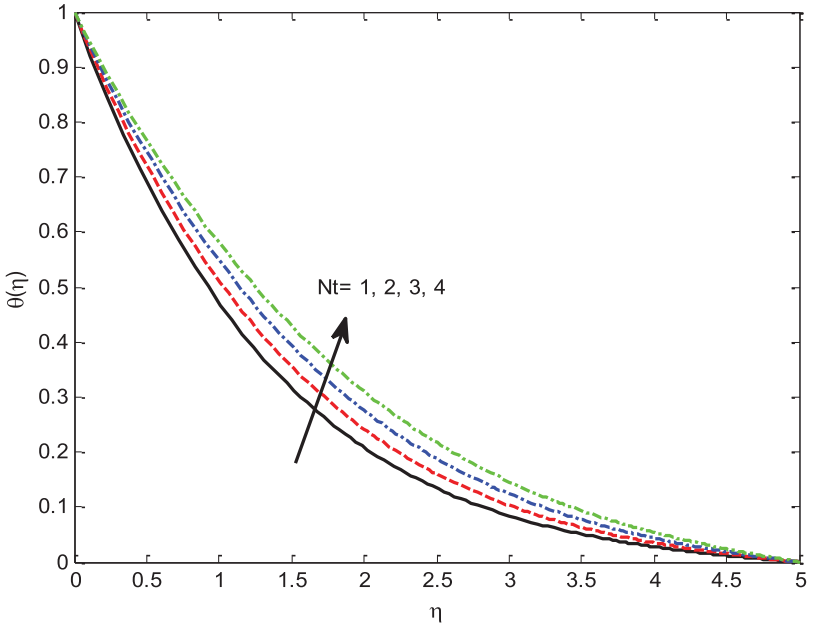

Figure 13. Effect of Nt on $\theta(\eta)$.

some limiting cases. From this table, we finalized that our outcomes and the numerical processes agree with the previous results. The numerical values of the skin friction coefficient, local Nusselt number and local Sherwood number are presented in Table 3. It is clear that the friction at the wall increases with increasing the values of M, A, and S. The skin friction

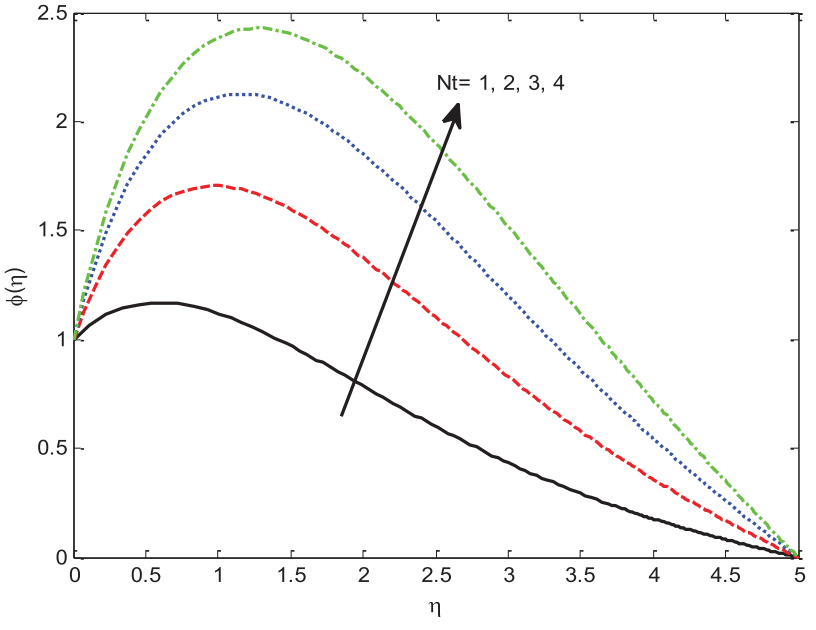

Figure 14. Effect of Nt on $\phi(\eta)$.

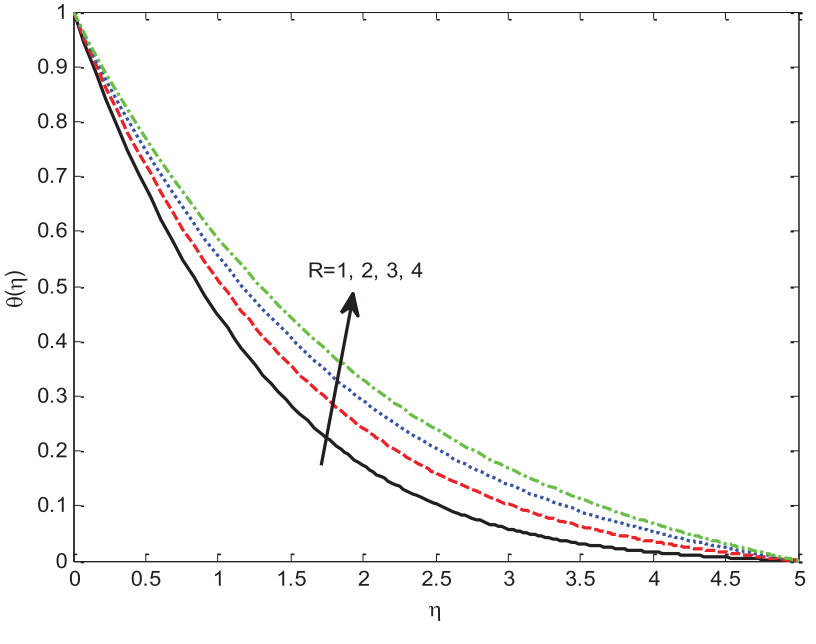

Figure 15. Effect of R on $\theta(\eta)$.

is found independent for A*, B*, R, Nt, Nb and *Sc*. The heat transfer rate is significantly depreciated by improving the values of M, A*, B*, R, Nt, Nb and *Sc*, while an opposite

Table 3. Numerical values of $f''(0)$, $-\left(\theta'(0)\left(1+\frac{4R}{3}\right)\right)$ and $-\phi'(0)$, for distinct flow parameters with $M = 2, B^* = -0.1, Pr = 0.71, S = 0.6, Nt = 0.3, Sc = 0.3, \eta = A = 0.5, A^* = Nb = 0.2, R = 0.5$.

M	A	$A*$	$B*$	R	Nt	Nb	Sc	S	$f''(0)$	$-\theta'(0)\left(1+\frac{4R}{3}\right)$	$-\phi'(0)$
1	–	–	–	–	–	–	–	–	2.090403	0.488387	0.423744
2	–	–	–	–	–	–	–	–	2.336726	0.478783	0.422673
3	–	–	–	–	–	–	–	–	2.557423	0.471089	0.422303
–	1	–	–	–	–	–	–	–	2.428908	0.767871	0.336451
–	2	–	–	–	–	–	–	–	2.578384	1.082399	0.354694
–	3	–	–	–	–	–	–	–	2.696406	1.288572	0.406001
–	–	−0.1	–	–	–	–	–	–	2.336726	0.614367	0.240171
–	–	0	–	–	–	–	–	–	2.336726	0.569188	0.300984
–	–	0.1	–	–	–	–	–	–	2.336726	0.523993	0.361818
–	–	–	0.1	–	–	–	–	–	2.336726	0.700974	0.151542
–	–	–	0.2	–	–	–	–	–	2.336726	0.600675	0.275598
–	–	–	0.3	–	–	–	–	–	2.336726	0.478783	0.422673
–	–	–	–	1	–	–	–	–	2.336726	0.403636	0.510826
–	–	–	–	2	–	–	–	–	2.336726	0.332097	0.593417
–	–	–	–	3	–	–	–	–	2.336726	0.297691	0.632675
–	–	–	–	–	1	–	–	–	2.336726	0.437503	−0.16180
–	–	–	–	–	2	–	–	–	2.336726	0.386413	−0.67598
–	–	–	–	–	3	–	–	–	2.336726	0.343362	−0.90854
–	–	–	–	–	–	1	–	–	2.336726	0.407437	0.696487
–	–	–	–	–	–	2	–	–	2.336726	0.332602	0.728706
–	–	–	–	–	–	3	–	–	2.336726	0.271795	0.738155
–	–	–	–	–	–	–	0.1	–	2.336726	0.485512	0.029549
–	–	–	–	–	–	–	0.2		2.336726	0.481616	0.242270
–	–	–	–	–	–	–	0.3		2.336726	0.478783	0.422673
–	–	–	–	–	–	–	–	1	2.557755	0.579826	0.345578
–	–	–	–	–	–	–	–	2	3.188323	0.883227	0.064207
–	–	–	–	–	–	–	–	3	3.914735	1.231997	−0.28468

behavior is observed on A and S. i.e. the suction parameter will increase the heat transfer rate between particles to the surface. Further, the mass transfer rate shows significant variation towards involved flow parameters.

5. Concluding remarks

The effect of non-uniform heat sink or source on heat transfer is another significant aspect in the outlook of numerous physical problems. Heat generation or absorption may alter fluid heat distribution, which consequently affects the rate of particle deposition in electronic devices and nuclear reactors. Heat source or sink may be assumed as fixed or space and temperature-dependent parameters. With this purpose, we aimed to discuss the influence of non-uniform heat sources or sink on unsteady nanofluid flow through an exponentially stretching sheet with consideration of the thermal radiation effect. The major findings of our study are:

- We noted that nanofluid temperature is enhanced for heat generation parameter and reduced for heat absorption parameter.
- The fluid velocity decreases with the rising values of a suction parameter
- A stronger magnetic field causes to increase the heat diffusion. Therefore, the heat transfer rate is decreased.

- In absolute sense, the skin friction increases as magnetic field increases. Further, the magnitude is larger for magnetic field flow.
- The Brownian motion and thermophoresis parameters significantly enhanced the nanofluid temperature. Since Brownian motion plays an important role in the enhancement of thermal conductivity of nanofluids.
- An increase in radiation parameter gives way to extreme heating to the nanofluid that causes to escalate the temperature and boundary layer thickness.
- The present framework can be extended to evaluate the flow analysis of water-based nanofluids over different geometries having engineering standpoints.

Acknowledgement

The authors would like to thank Prince Sultan University for their support through the TAS research lab.

Disclosure statement

No potential conflict of interest was reported by the author(s).

References

[1] Sakiadis BC. Boundary-layer behavior on continuous solid surfaces: I. boundary-layer equations for two-dimensional and axisymmetric flow. AIChE J. 1961;7(1):26–28.
[2] Erickson LE, Fan LT, Fox VG. Heat and mass transfer on moving continuous flat plate with suction or injection. Ind Eng Chem Fundam. 1966;5(1):19–25.
[3] Carragher P. Heat transfer on a continuous stretching sheet. Z Angew Math Mech. 1982;62: 564–565.
[4] Grubka LJ, Bobba KM. Heat transfer characteristics of a continuous stretching surface with variable temperature. J Heat Transfer. 1985;107(1):248–250.
[5] Magyari E, Keller B. Heat and mass transfer in the boundary layers on an exponentially stretching continuous surface. J Phys D: Appl Phys. 1999;32(5):577.
[6] Mabood F, Khan WA, Md Ismail AI. MHD flow over exponential radiating stretching sheet using homotopy analysis method. J King Saud Univ-Eng Sci. 2017;29(1):68–74.
[7] Mukhopadhyay S. MHD boundary layer flow and heat transfer over an exponentially stretching sheet embedded in a thermally stratified medium. Alexandria Eng J. 2013;52(3):259–265.
[8] Hayat T, Shafiq A, Alsaedi A, et al. Unsteady MHD flow over exponentially stretching sheet with slip conditions. Appl Math Mech. 2016;37(2):193–208.
[9] Ahmad K, Hanouf Z, Ishak A. Mixed convection Jeffrey fluid flow over an exponentially stretching sheet with magnetohydrodynamic effect. AIP Adv. 2016;6(3):035024.
[10] Seini YI, Makinde OD. MHD boundary layer flow due to exponential stretching surface with radiation and chemical reaction. Math Probl Eng. 2013;2013:1–7. doi:10.1155/2013/163614.
[11] Partha MK, Murthy PVSN, Rajasekhar GP. Effect of viscous dissipation on the mixed convection heat transfer from an exponentially stretching surface. Heat Mass Transfer. 2005;41(4):360–366.
[12] Ishak A. MHD boundary layer flow due to an exponentially stretching sheet with radiation effect. Sains Malaysiana. 2011;40(4):391–395.
[13] Jat RN, Chand G. MHD flow and heat transfer over an exponentially stretching sheet with viscous dissipation and radiation effects. Appl Math Sci. 2013;7(4):167–180.
[14] Choi SUS, Eastman JA. Enhancing thermal conductivity of fluids with nanoparticles. No. ANL/MSD/CP-84938; CONF-951135-29. Argonne National Lab.(ANL), Argonne, IL (United States), 1995.
[15] Buongiorno J. Convective transport in nanofluids. J. Heat Transfer. 2006;128(3):240–250.

[16] Tiwari RK, Das MK. Heat transfer augmentation in a two-sided lid-driven differentially heated square cavity utilizing nanofluids. Int J Heat Mass Transfer. 2007;50(9–10):2002–2018.
[17] Nadeem S, Lee C. Boundary layer flow of nanofluid over an exponentially stretching surface. Nanoscale Res Lett. 2012;7(1):1–6.
[18] Mustafaa M, Hayat T, Obaidat S. Boundary layer flow of a nanofluid over an exponentially stretching sheet with convective boundary conditions. Int J Numer Methods Heat Fluid Flow. 2013;23:945–959.
[19] Nadeem S, Haq RU, Khan ZH. Heat transfer analysis of water-based nanofluid over an exponentially stretching sheet. Alexandria Eng J. 2014;53(1):219–224.
[20] Bhattacharyya K, Layek GC. Magnetohydrodynamic boundary layer flow of nanofluid over an exponentially stretching permeable sheet. Phys Res Int. 2014;2014:1–12.
[21] Anwar I, Shafie S, Salleh MZ. Radiation effect on MHD stagnation-point flow of a nanofluid over an exponentially stretching sheet. Walailak J Sci Technol (WJST). 2014;11(7):569–591.
[22] Loganathan P, Vimala C. MHD boundary layer flow of a nanofluid over an exponentially stretching sheet in the presence of radiation. Heat Transf–Asian Res. 2014;43(4):321–331.
[23] Hayat T, Imtiaz M, Alsaedi A, et al. MHD flow of nanofluids over an exponentially stretching sheet in a porous medium with convective boundary conditions. Chin Phys B. 2014;23(5):054701.
[24] Mohamed RA, Rida SZ, Mubarak MS. MHD nanofluid flow over an exponentially radiating stretching sheet through a porous medium with suction/injection. J Nanofluids. 2016;5(2):273–283.
[25] Foraboschi FP, Di Federico I. Heat transfer in laminar flow of non-newtonian heat-generating fluids. Int J Heat Mass Transfer. 1964;7(3):315–325.
[26] Shahzad F, Baleanu D, Jamshed W, et al. Flow and heat transport phenomenon for dynamics of Jeffrey nanofluid past stretchable sheet subject to Lorentz force and dissipation effects. Sci Rep. 2021;11(1):1–15.
[27] Shamshuddin MD, Eid MR. Magnetized nanofluid flow of ferromagnetic nanoparticles from parallel stretchable rotating disk with variable viscosity and thermal conductivity. Chin J Phys. 2021;74:20–37.
[28] Amine BM, Redouane F, Mourad L, et al. Magnetohydrodynamics natural convection of a triangular cavity involving Ag-MgO/water hybrid nanofluid and provided with rotating circular barrier and a quarter circular porous medium at its right-angled corner. Arab J Sci Eng. 2021;46(12):12573–12597.
[29] Boumaiza N, Kezzar M, Eid MR, et al. On numerical and analytical solutions for mixed convection Falkner-Skan flow of nanofluids with variable thermal conductivity. Waves Random Complex Media. 2021;31(6):1550–1569.
[30] Waqas H, Hussain M, Alqarni MS, et al. Numerical simulation for magnetic dipole in bioconvection flow of Jeffrey nanofluid with swimming motile microorganisms. Waves Random Complex Media. 2021: 1–18. doi:10.1080/17455030.2021.1948634.
[31] Bhattacharyya K, Pop I. MHD boundary layer flow due to an exponentially shrinking sheet. Magnetohydrodynamics. 2011;47(4):337–344.
[32] Pal D. Combined effects of non-uniform heat source/sink and thermal radiation on heat transfer over an unsteady stretching permeable surface. Commun Nonlinear Sci Numer Simul. 2011;16(4):1890–1904.
[33] Kumar RK, Vijaya Kumar Varma S. Stagnation point flow of thermally radiative and dissipative MHD nanofluid over a stretching sheet filled with porous medium and suction. Songklanakarin J Sci Technol. 2019;41:123–135.
[34] Hymavathi T, Mathews J, Kiran Kumar RVMSS. Heat transfer and inclined magnetic field effects on unsteady free convection flow of MoS_2 and MgO–water based nanofluids over a porous stretching sheet. Int J Ambient Energy. 2021: 1–9. doi:10.1080/01430750.2021.1995491.
[35] Abd El-Aziz M. Viscous dissipation effect on mixed convection flow of a micropolar fluid over an exponentially stretching sheet. Can J Phys. 2009;87(4):359–368.
[36] Mukhopadhyay S. Slip effects on MHD boundary layer flow over an exponentially stretching sheet with suction/blowing and thermal radiation. Ain Shams Eng J. 2013;4(3):485–491.

[37] Redouane F, Jamshed W, Suriya Uma Devi S, et al. Galerkin finite element study for mixed convection (TiO_2–SiO_2/water) hybrid-nanofluidic flow in a triangular aperture heated beneath. Sci Rep. 2021;11:1–15.
[38] Shamshuddin MD, Abderrahmane A, Koulali A, et al. Thermal and solutal performance of Cu/CuO nanoparticles on a non-linear radially stretching surface with heat source/sink and varying chemical reaction effects. Int Commun Heat Mass Transfer. 2021;129:105710.
[39] Jamshed W, Prakash M, Devi S, et al. A brief comparative examination of tangent hyperbolic hybrid nanofluid through a extending surface: numerical Keller–Box scheme. Sci Rep. 2021;11:1–32.
[40] Jamshed W, Shahzad F, Safdar R, et al. Implementing renewable solar energy in presence of Maxwell nanofluid in parabolic trough solar collector: a computational study. Waves Random Complex Media. 2021: 1–32. doi:10.1080/17455030.2021.1989518.
[41] Al-Hossainy AF, Eid MR. Combined theoretical and experimental DFT-TDDFT and thermal characteristics of 3-D flow in rotating tube of [PEG+ H_2O/SiO_2-Fe_3O_4] C hybrid nanofluid to enhancing oil extraction. Waves Random Complex Media. 2021: 1–26. doi:10.1080/17455030.2021.1948631.
[42] Rehman KU, Shatanawi W, Abodayeh K. Thermophysical aspects of magnetized williamson fluid flow subject to both porous and non-porous surfaces: A Lie symmetry analysis. Case Stud Therm Eng. 2021;28:101688.
[43] Eid MR, Al-Hossainy AF. Combined experimental thin film, DFT-TDDFT computational study, flow and heat transfer in [PG-MoS_2/ZrO_2] C hybrid nanofluid. Waves Random Complex Media. 2022: 1–26. doi:10.1080/17455030.2021.1873455.
[44] Rehman KU, Khan AU, Rehman F, et al. Thermal case study on linearly twisting cylinder: a radial stagnation point flow of nanofluid. Case Stud Therm Eng. 2022;31:101861.
[45] Rehman KU, Shatanawi W, Al-Mdallal QM. A comparative remark on heat transfer in thermally stratified MHD Jeffrey fluid flow with thermal radiations subject to cylindrical/plane surfaces. Case Stud Therm Eng. 2022:101913.